

## On the synthesis of micro-electromechanical filters using structural dynamics

To cite this article: A Elka and I Bucher 2008 *J. Micromech. Microeng.* **18** 125018

View the [article online](#) for updates and enhancements.

### You may also like

- [Ultra-wide bandstop infrared MIM filter using aperture coupled square cavities](#)  
Mehdi Kamari, Saba Khosravi and Mohsen Hayati
- [Inline selection of transmission or reflection spectra of different fiber Bragg gratings using polarization-diversity loop](#)  
Jihoon Kim, Hyun Wook Kang, Seung Yun Nam et al.
- [Ultra wideband bandstop plasmonic filter in the NIR region based on stub resonators](#)  
Imane Zegaar, Abdesselam Hocini, Hocine Bensalah et al.

**ECS**  
The  
Electrochemical  
Society  
Advancing solid state &  
electrochemical science & technology

**DISCOVER**  
how sustainability  
intersects with  
electrochemistry & solid  
state science research

# On the synthesis of micro-electromechanical filters using structural dynamics

A Elka and I Bucher

Mechanical Engineering, Technion, Israel institute of Technology, Haifa 32000, Israel

E-mail: [elka@technion.ac.il](mailto:elka@technion.ac.il) and [bucher@technion.ac.il](mailto:bucher@technion.ac.il)

Received 28 April 2008, in final form 4 September 2008

Published 6 November 2008

Online at [stacks.iop.org/JMM/18/125018](http://stacks.iop.org/JMM/18/125018)

## Abstract

This paper discusses a new synthesis approach for electromechanical filters. The structural dynamics aspects are emphasized and joined with an inverse problem methodology to shape the spectrum of a signal passing through the device. Using the inverse problem methodology, the poles and zeros of a multi-degree of freedom structure are assigned, thus shaping the filter's frequency response. Several variants are presented for the same topology where the excitation and sensing locations are chosen according to the desired characteristics of the filter. The decomposition of the spatial behaviour of the device provides the designer with the ability to suppress certain structural modes of vibration thus behaving as a bandstop/bandpass filter for periodic signals. A micro-electromechanical filter was fabricated and a laboratory set-up was constructed for characterization of the micro-electromechanical filter. A comparison between the simulated response of the filter and measured response is shown.

## 1. Introduction

Electromechanical filters have recently received more attention with the appearance of micro-electromechanical (MEMS) structures. The reason behind the rapid development and then adaptation of the mechanical filter is its superior characteristics, including a high quality factor, good temperature stability and ageing properties, which are all critical in achieving low-loss, narrow bandwidth, and high stability filters [1]. These devices can be incorporated on a chip level basis with the surrounding electronics, and this makes them rather attractive [2, 3].

Filters as a unit receive an electrical signal and after shaping its spectrum, i.e. modifying the signal by affecting its amplitude and phase over selected ranges of frequency [4], the mechanical stress waves or deformations are converted back to electromechanical signals. In electromechanical filters, the input signal is converted into oscillating mechanical deformations, the mechanical structure is designed such that it performs the necessary spectrum shaping and finally the mechanical oscillations or waves are converted back into an electrical signal [2, 3, 5]. Indeed, MEMS oscillators and filters have attracted a number of publications; some recent developments and concepts can be found in [6, 7].

These references, as well as many others, have exploited the dynamics and more specifically the modes of vibration of structures with (effectively) up to three degrees of freedom.

The conceptual design that was investigated so far mainly comes from classical electric filter theory [4, 8]. An analog filter circuit consists of a single input and single output. This topology is often called a two-port network. Different configurations of mechanical filters can be found in the literature:

In [9], a single clamped-clamped resonator in lateral vibration is described. In [7], two clamped-clamped micro-resonators are coupled together with a soft flexural-mode coupling beam.

Hence, higher order systems with multiple-coupling springs enable synthesis of high-quality filters. Highly selective RF filters between antenna and preamplifier make sure that only signals from the correct receiver band will be amplified. Ways of realizing high-order filters are described in [6], three comb-drive resonators are coupled together with a flexural coupling beam, creating a third-order MEMS filter. A method for realizing a fourth-order micromechanical filter using a disk resonator [10, 11] was tested. In [12], up to 20 drumhead resonators were coupled

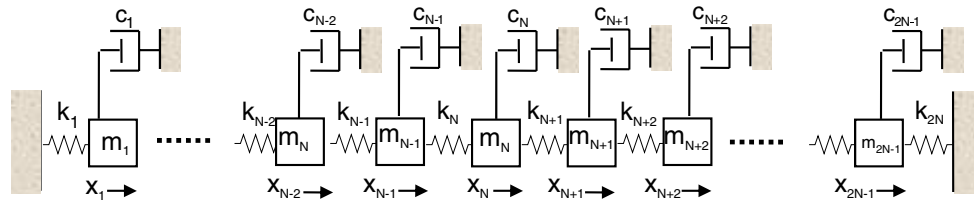


Figure 1. Symmetric spring–mass and damper system.

and their theoretical and experimental behaviour was studied. The effect of inter-coupling was discussed. In [3], a series of micromechanical filters which link two adjacent resonators and springs is configured to have an improved bandpass characteristic by a proper selection of mass and stiffness. A bridged micromechanical filter is presented in [13]. The filter design utilizes coupling bridging springs to achieve a low insertion loss frequency shaping transfer function with sharper roll-offs.

In order to improve the performance of these devices, higher order filters should be used [8]. To fulfil this task, concepts taken from structural dynamics and modal-testing are being employed since current methods are capable of designing relatively low order micromechanical filters (see, for example, [6, 7]). A multi-degree of freedom topology for a mechanical filter is tailored here to possess superior dynamical behaviour that can produce higher order filters with improved characteristics (such as sharp roll off, better stop-band rejection). This topology can be operated with several different combinations of actuation and sensing locations. Damping can be applied at certain spatial locations according to the desired behaviour of this system using mechanical, fluid (squeeze-film [14]) or external electrical means [15]. Each of these actuation/sensing combinations can create, for the same mechanical filter design, a unique spectral shaping.

The performance of filters relies on the obtainable accuracy of the natural frequencies. The small dimensions and the limitations of the presently available MEMS manufacturing methods force the designers to employ tuning methods or use error compensation techniques [16]. Another delicate point is related to the controlled resistive or dissipative response. Dissipation can be employed by regulating the gap between two vibrating surfaces [5, 14] or by employing an external force–feedback electrical circuit [15].

A mechanical filter is in fact a dynamical system whose behaviour can be tailored by an optimization process [17], but when narrow band processes are involved, the assignment of eigenvectors and eigenvalues seems more intuitive. In [18], a method to assign natural frequencies and eigenvectors by structural modifications is proposed. In the current application, it seems more suitable to rely on methods where the entire stiffness and mass distribution alongside the topology are found from the mechanical filter characteristics. In this case, it was chosen to use an inverse vibration problem such as the one described in [16, 19–21]. In particular the construction method that was described in [20] is being used whereby an exact solution can be found for a particular problem of natural frequency assignment [20].

This work seeks to emphasize the role of an appropriate analysis of the mechanical filter. The analysis shown here can accommodate any number of degrees of freedom in contradiction to the usual lumped modelling in terms of an electrical circuit via the exploitation of mechanical–electrical analogies and conveniently implemented in a circuit simulator.

The structure of the paper is as follows: first the theory of the relevant inverse problem is introduced, then the theoretical simulations of a mechanical filter are presented followed by some experimental results of a laboratory MEMS filter. Finally a method to control the bandwidth of a filter using a variation of the proposed inverse problem is described.

## 2. Spectrum shaping by tailoring a spring–mass series' topology

Filters are frequency selective devices that can be described by means of the filter's transfer function expressed by the poles and zeros. Controlling the latter parameters gives one the ability to design multi-degrees of freedom structures (MDOF) leading to a system with the desired properties.

This section introduces sub-cases of the general system outlined in figure 1. These sub-cases have different combinations of poles and zeros, where each combination gives rise to a different type of filtering operation, thus we can achieve and demonstrate an electromechanical filter for signal processing of periodic signals. We design the filter using a tool which is a general lumped modelling approach, although it is understood that the structure has an infinite number of modes. Still, a group of modes can be described by a limited number of lumped masses and springs while there is a group involving higher order deformations that is far beyond this frequency range. In practice, the lumped model can be used to refine the initial design [16] and later a detailed analysis is conducted to assure that the remaining flexible modes are well out of the frequency band of interest.

The analytical work presented in [20] is expanded here to make use of a similar construction of a MEMS scanning mirror [19] for a mechanical filter design.

Two cases are analysed here: in the first case, the excitation (input) acts on the first mass while the response (output) is on the last mass. In this case, the structure has no zeros and therefore there will not be any frequency in this range at which a significant attenuation of the signal will occur. With this design, the width of a bandpass filter can be increased as will be shown later. The second case deals with a structure where both the excitation and response are the central mass. In this case, there will be zeros (as proved below) between

every pair of poles. This construction is adapted here for the filtration of periodic signals, by instructing notch or high- $Q$  filters.

Consider a MDOF vibrating system consisting of a spring ( $k$ ), mass ( $m$ ) and damper ( $c$ ) connected in series; this system is schematically illustrated in figure 1.

The system has  $(2N - 1)$  degrees of freedom and it is symmetric around the centre of mass ( $m_N$ ). The symmetry of the proposed topology defines that  $m_i = m_{2N-i}, k_i = k_{2N-i+1}, i = 1, \dots, N$ .

This system has two types of eigenvectors (mode shapes): symmetric and anti-symmetric. The asymmetric modes exhibit zero motion at the central mass. Furthermore, it was shown in [20] that the point receptance of the middle degree of freedom (DOF) has anti-resonance (zeros) at the even numbered natural frequencies. The symmetry of the proposed topology can be used to convert the problem into two smaller problems [20, 21]: problem one represents the symmetric vibration modes and problem two represents the asymmetric ones. The eigenvalues paired with the symmetric modes of this matrix are known to be distinct, maintaining  $0 < \lambda_1 < \lambda_2 < \dots < \lambda_N$  that represent the natural frequencies (poles). For the asymmetric modes the modified eigenvalue problem has eigenvalues that are  $\mu = \mu_k, k = 1, \dots, N - 1$  which represent the anti-resonance frequencies (zeros). It is well known from system theory that the response to an excitation at the same location contains the strict interlacing property  $\lambda_k < \mu_k < \lambda_{k+1}$ . Each frequency is associated with a particular pole/zero or resonance/anti-resonance and the associated eigenvector (mode shape) is at the relevant frequency.

The topology of the vibrating system is found from a dedicated inverse problem which was described in [20, 21] by which a spring-mass system is reconstructed to have a specified spectrum with prescribed natural frequencies/vibration modes [21, 22].

The mathematical model involves matrices whose spectral properties determine the dynamics of the physical system.

For a serially linked mass-spring system with  $N$  masses, fixed at both ends, the equations of motion are given by

$$\begin{bmatrix} m_1 & & & & \\ & m_1 & & & \\ & & \ddots & & \\ & & & \ddots & \\ & & & & m_N \end{bmatrix} \begin{pmatrix} \ddot{x}_1 \\ \ddot{x}_2 \\ \vdots \\ \ddot{x}_N \end{pmatrix} + \begin{bmatrix} k_1 + k_2 & -k_2 & & & \\ -k_2 & k_2 + k_3 & -k_3 & & \\ & & \ddots & \ddots & \\ & & & -k_N & \\ & & & -k_N & k_N + k_{N+1} \end{bmatrix} \begin{pmatrix} x_1 \\ x_2 \\ \vdots \\ x_N \end{pmatrix} = 0. \quad (1)$$

Abbreviated in matrix form as

$$\mathbf{M}\ddot{\mathbf{x}} + \mathbf{K}\mathbf{x} = 0, \quad (2)$$

where  $\mathbf{K}$  is a Jacobi, tridiagonal symmetric matrix.

Using a coordinate transformation

$$\mathbf{x} = \mathbf{M}^{-1/2}\mathbf{u} \quad (3)$$

to obtain

$$(\mathbf{B} - \lambda\mathbf{I})\mathbf{u} = 0 \quad (4)$$

and a tri-diagonal equation of motion

$$\ddot{\mathbf{u}} + \mathbf{B}\mathbf{u} = 0, \quad (5)$$

where  $\mathbf{B} = \mathbf{M}^{-1/2}\mathbf{K}\mathbf{M}^{-1/2}$ , thus

$$\mathbf{B} = \begin{pmatrix} a_1 & -b_1 & 0 & \dots & 0 & 0 \\ -b_1 & a_2 & -b_2 & \dots & 0 & 0 \\ \vdots & & & & & \vdots \\ 0 & 0 & 0 & \dots & a_{N-1} & -b_{N-1} \\ 0 & 0 & 0 & \dots & -b_{N-1} & a_N \end{pmatrix}, \quad (6)$$

where  $\mathbf{B}$  is a tri-diagonal Jacobian matrix. The eigenvalues of a Jacobi matrix are necessarily real and distinct [21]. The actual mass and stiffness values can be reconstructed from the Jacobi matrix. To perform this reconstruction the Lanczos algorithm is being used [21]. A detailed computer program and a formal mathematical derivation for reconstructing the matrix from prescribed spectral data are given in [20]. It has been shown that the structure is scalable in the frequency domain [16, 20], thus none of the eigenvectors depends on the minimal actual frequency,  $\omega_0$ . The basis frequency can be obtained from the general solution by means of scaling only [16, 20].

Two cases are being proved here. One concerns the case where the excitation and sensing taking place on the first and last masses, respectively. The second deals with excitation and sensing residing at the central mass. The selected cases have physical meaning in shaping a frequency response function by assigning and controlling the poles and zeros to obtain a desired filter for signal processing.

The mass and stiffness matrices that represent the system in figure 1 (neglecting the damping), are

$$\mathbf{M} = \begin{bmatrix} m_1 & 0 & \dots & 0 \\ 0 & m_2 & \ddots & \vdots \\ \vdots & \ddots & \ddots & 0 \\ 0 & \dots & 0 & m_{2N-1} \end{bmatrix},$$

$$\mathbf{K} = \begin{bmatrix} k_1 + k_2 & -k_2 & \dots & 0 \\ -k_2 & k_2 + k_3 & \ddots & \vdots \\ \vdots & \ddots & \ddots & -k_{2N-1} \\ 0 & \dots & -k_{2N-1} & k_{2N-1} + k_{2N} \end{bmatrix}$$

$$\in \mathbb{R}^{(2N-1) \times (2N-1)}. \quad (7)$$

With these definitions, it is now possible to develop an expression for the receptance in two cases. Case 1 deals with the point receptance of the middle mass and case 2 treats the receptance where the force is applied at one end of the structure and the response is measured at the other end.

We denote the receptance of the former as

$$\frac{x_1}{f_{2N-1}}(\omega) = e_1^T (\mathbf{K} - \omega^2\mathbf{M})^{-1} e_{2N-1}, \quad (8)$$

where  $e_n$  is the  $n$ th column of the  $(2N - 1) \times (2N - 1)$  identity matrix, while the point receptance at the middle mass as

$$\frac{x_N}{f_N}(\omega) = e_N^T (\mathbf{K} - \omega^2\mathbf{M})^{-1} e_N. \quad (9)$$

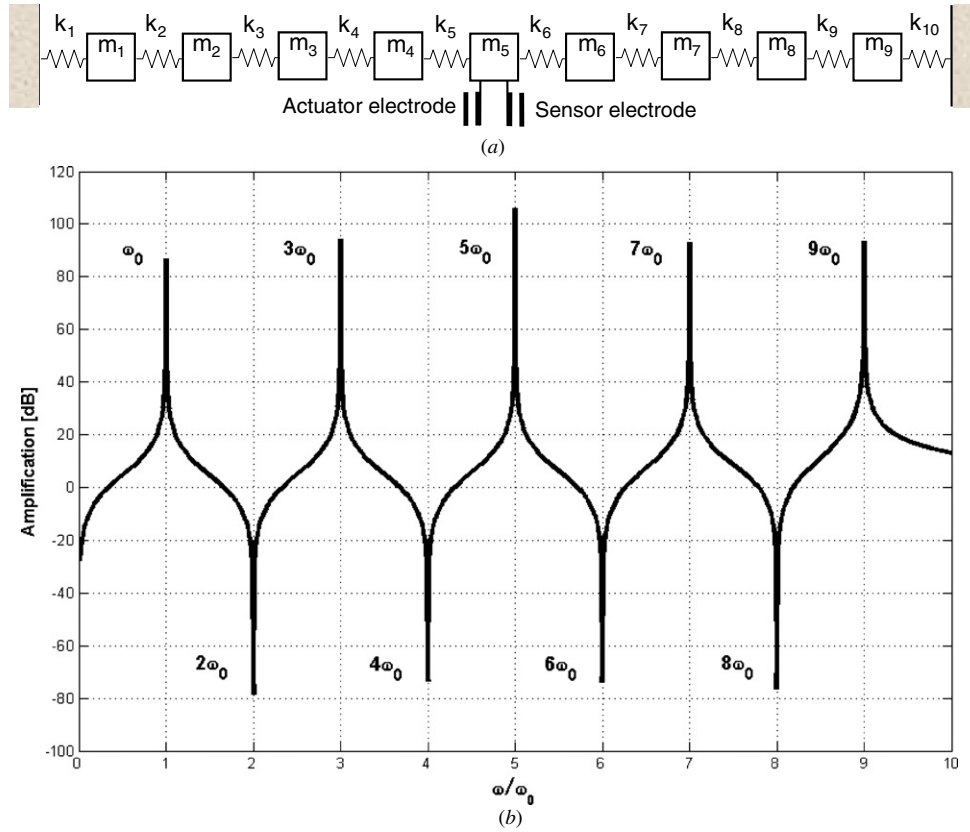


**Figure 2.** (a) A nine degrees of freedom series spring–mass system. (b) Response magnitude of the central mass in a nine DOF system versus frequency.

The main thrust of this paper is the ability to selectively assign poles and zeros to the mechanical filter. This section shows that poles and zeros can indeed be placed at the correct regions in the frequency domain. Two brief proofs are brought below as an aid.

Proof that  $\frac{x_1}{f_{2N-1}}(\omega)$  has no zeros

$$\frac{x_1}{f_{2N-1}}(\omega) = \frac{e_1^T \text{adj}(\mathbf{K} - \omega^2 \mathbf{M}) e_{2N-1}}{\det(\mathbf{K} - \omega^2 \mathbf{M})}. \quad (10)$$

We can calculate the adjoint of the dynamical matrix in (10) using the matrix of minors and cofactors, thus the numerator of the transfer function,  $e_1^T \text{adj}(\mathbf{K} - \omega^2 \mathbf{M}) e_{2N-1}$ , is equal to

$$\det \begin{bmatrix} -k_2 & k_2 + k_3 - \omega^2 m_2 & -k_3 \\ 0 & \ddots & \\ 0 & 0 & -k_{2N-2} \end{bmatrix} = k_2 k_3 \cdots k_{2N-2} (-1)^{2N-2}. \quad (11)$$

The determinant of the upper triangle matrix is the product of the diagonal terms; these terms are constants only, thus there are no zeros in the transfer function.

Proof that  $\frac{x_N}{f_N}(\omega)$  has the strict interlacing property.

References [20, 22] prove the property of interlacing poles and zeros through a Sturm polynomial for the case of collocation receptance.

### 3. Simulated electromechanical filter examples

For generality we selected arbitrarily a nine degrees of freedom based design as an example. The system has a high compliance at the odd multiples of frequencies, schematically shown in figure 2(a). The new design topology can be tuned to have a large amplification of the excitation voltage at frequencies  $\omega_0, 3\omega_0, 5\omega_0, 7\omega_0, 9\omega_0$  and an extremely high attenuation at  $2\omega_0, 4\omega_0, 6\omega_0, 8\omega_0$ , figure 2(b).

The damping level can be controlled by a feedback electric network [15] to selectively attenuate the vibrating amplitudes as shown in figure 3. A second approach to controlling the damping, but more sensitive to temperature variations, would use the squeeze-film effect of the air trapped between one of the masses and a flat surface in close proximity [14]. For small vibrations as expected in the present application, the damping due to the squeeze-film effect is linear and its value can be determined by designing the geometry of the damper.

Electromechanical feedback or force balancing transducer allows precise control of the  $Q$  of the constituent resonators, independent of the ambient operating pressure (and temperature) fluctuations of the micromechanical system.

The detection (sensor) mechanism exploits the fact that, because the mechanical vibration makes the structure exhibit a time varying capacitance (change in charge), it can be detected as a current flow ( $i$ ) by means of a charge amplifier. The current flow through the resistor ( $R_L$ ) thus creates a voltage drop on it. The difference between the output

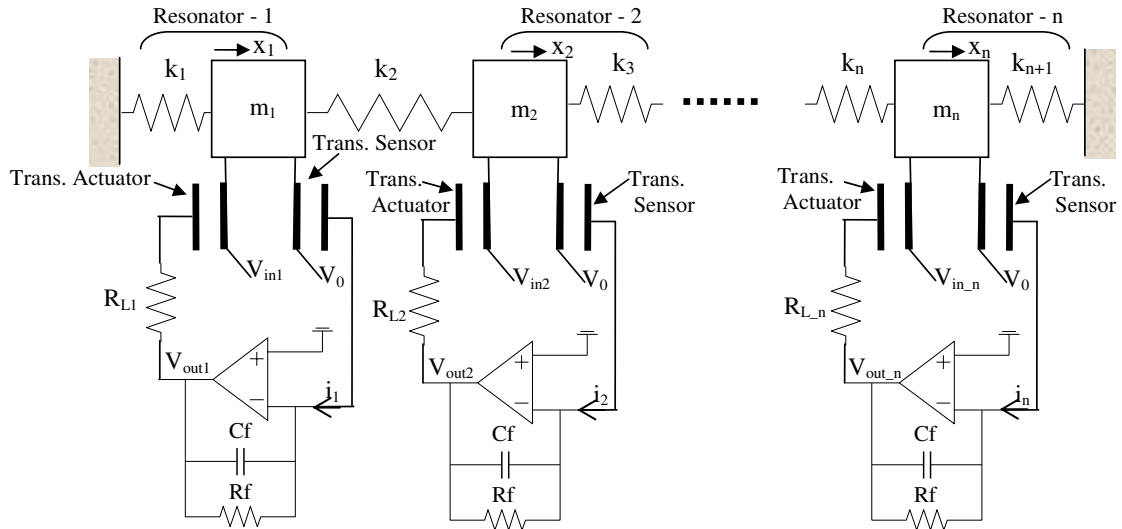


Figure 3. Schematic of damping control by an electric network.

voltage of the charge amplifier and the voltage on the resistor is fed back to the actuation capacitor. This generates an electrostatic force which is proportional to the mass velocity and which always opposes motion of the mass from the rest position. This dissipation is equivalent to a mechanical viscous damper.

It is possible to control the  $Q$  factor of the resonator system ( $Q$  of the order 1000) and attenuate the natural frequencies.

In addition, spectral shaping can be achieved by changing the excitation and sensing positions as this moves the zeros of the individual transfer functions. For the same structure, several unique spectral shapes can be formed, depending on the spatial actuation/sensing/damping properties of the structure.

Throughout this paper, it is assumed that the structure is designed such that it is effectively an  $(2N - 1)$ -DOF structure (large masses connected by thin springs). All the  $(2N - 1)$  modes of vibration are accounted for in the design and analysis. Evidently, since it is a continuum there would be many more modes of vibration, but when designed properly, these modes (where the inertia of the thin connecting springs becomes significant) would have natural frequencies that are much higher than the ‘operating range’ where the first  $(2N - 1)$  natural frequencies reside. Being so much higher, these modes are easily filtered out using the simplest of filters ( $RC$ ).

Some examples of the abovementioned symmetric nine DOF vibrating system are shown below to demonstrate the new filter synthesis methodology.

### 3.1. Example 1. Notch filter for periodic signals

A nine DOF system with natural frequencies that are odd multiple frequencies of  $\omega_0 = 1 \text{ MHz}$  ( $\omega_{2n-1} = (2n - 1)\omega_0$ ,  $n = 1, 2, 3, \dots$ ) and anti-resonances (zeros) at even frequencies ( $\omega_{2n} = 2n\omega_0$ ,  $n = 1, 2, 3, \dots$ ) was designed by employing the algorithm in [20]. The actuation and sensing of the system are on the central mass ( $m_5$ ), and it is performed

by separate parallel electrodes. This system is shown in figure 4(a).

The general mode shapes in this system obey

$$\phi_{\text{asym}} = (\alpha_1 \ \alpha_2 \ 0 \ -\alpha_2 \ -\alpha_1)^T,$$

$$\phi_{\text{sym}} = (\beta_1 \ \beta_2 \ \beta_3 \ \beta_2 \ \beta_1)^T.$$

With damping acting on the central mass ( $m_5$ ) by an electrical dissipative network, it is possible to control the  $Q$  factor. In a different approach, a flat surface can be placed in close proximity to the middle mass thus increasing the squeeze-film effect until the desired level of damping is formed [14]. Indeed, the general form of the modes implies that attenuation of energy takes place on the symmetric modes only. Consequently, these modes can be ‘flattened’ completely, as shown in figures 4(b) and (c). A typical response of this filter is illustrated in figure 5.

Evidently, the symmetric topology has helped with complete flattening of the response at the odd natural frequencies while creating narrow bandstops at even multiples of the basis frequency.

### 3.2. Example 2. High- $Q$ multiple selective filter for signals with even periodic frequencies

In this example, the actuation of the system is on mass ( $m_1$ ) and the sensing is on mass ( $m_9$ ), the damping is acting on the central mass ( $m_5$ ), as shown in figure 6.

A typical response of this filter is illustrated in figure 7. This system configuration has no zeros according to the proof given in the section above. This type of filter will pass certain periodic signals while attenuating any other frequency contents.

It can be observed that the damping implies, in this case, attenuation on the symmetric modes of the system and therefore the corresponding frequencies are not amplified.

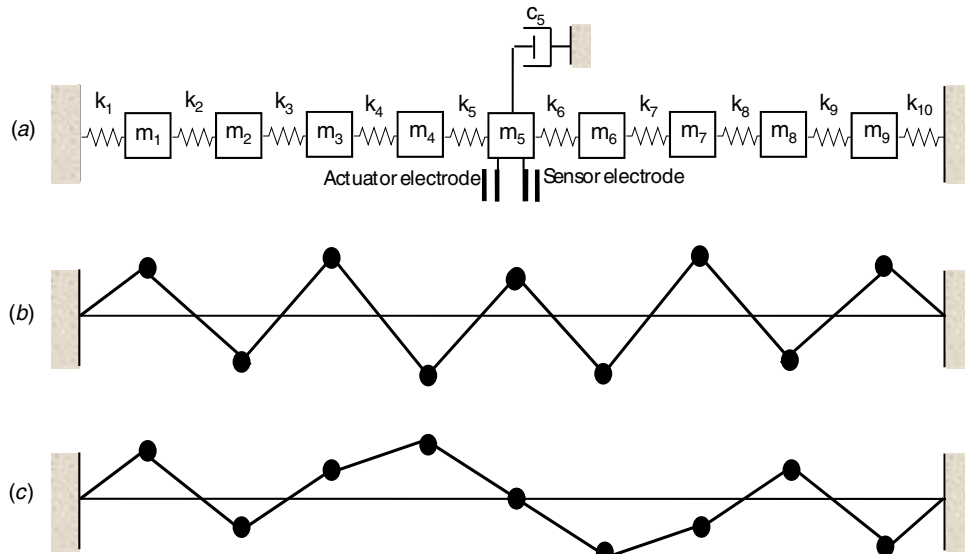


Figure 4. (a) Schematic of MDOF mechanical filter. (b) A typical symmetric mode. (c) A typical anti-symmetric mode.

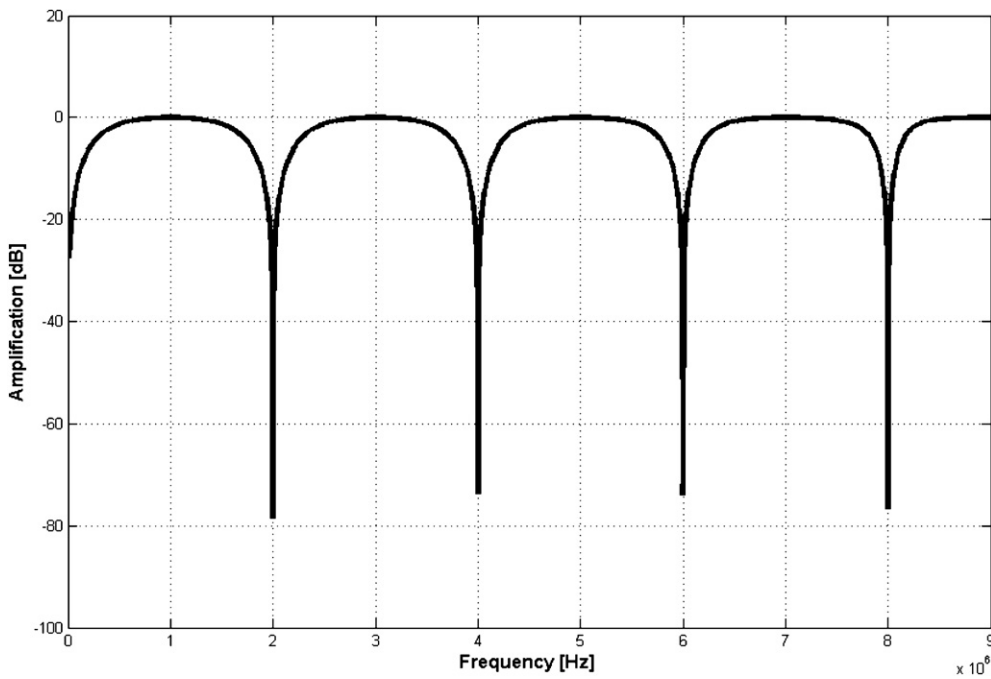


Figure 5. Response of a MDOF mechanical notch filter.

3.3. Example 3. High-Q multiple selective filter for signals with odd periodic frequencies

This example uses the actuation on mass ( $m_1$ ) and the sensing on mass ( $m_5$ ). Here no dissipation mechanism is introduced, as shown in figure 8.

A typical response of this filter is provided in figure 9 for periodic signals having energy with periodic multiples of 1 MHz.

The anti-symmetric modes of the system are filtered out in this case due to the configuration of actuation/sensing.

It has been shown that one can obtain reconfigurable filter characteristics using the same basic structure by choosing the excitation, response and damping-attachment locations.

4. MEMS filter device with five masses—experiment

To support the abovementioned examples, a MEMS structure acting as a filter device was designed and manufactured. Several experiments were performed to examine the validity of the design algorithm.

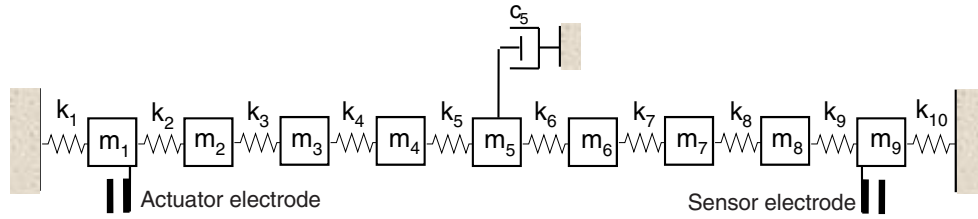


Figure 6. Schematic of a MDOF mechanical bandpass filter for even frequencies.

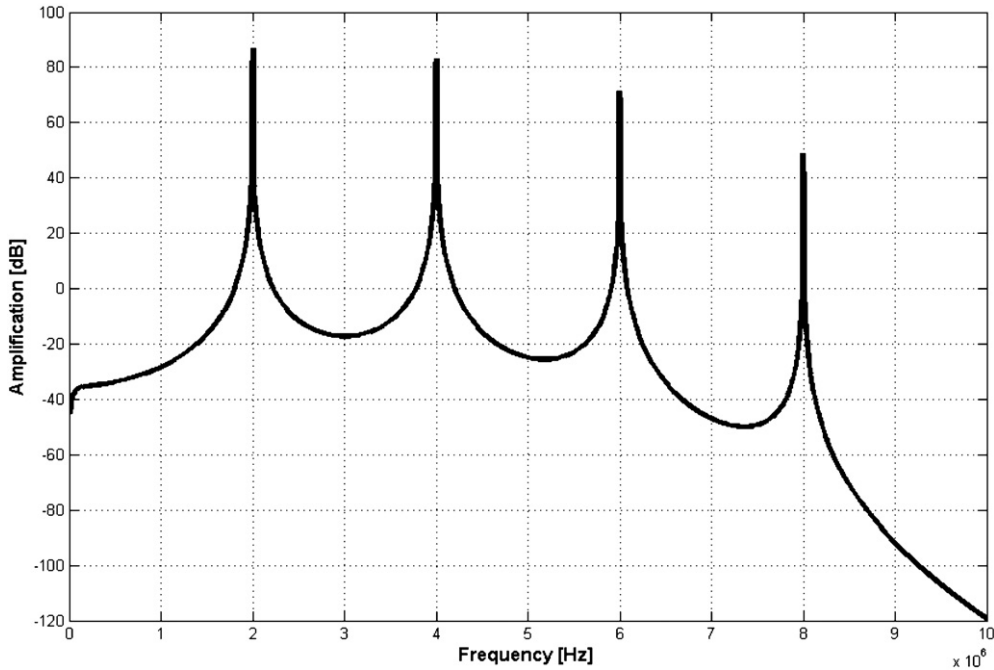


Figure 7. High-Q multiple selective filter for even frequencies.

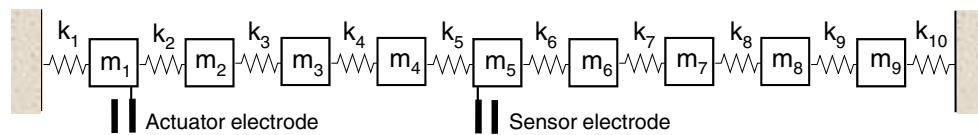


Figure 8. Schematic of MDOF mechanical bandpass filter for odd frequencies.

A five degree of freedom symmetric structure around the central mass was designed. The mechanical filter device is operating in torsion and is driven by spatial electrostatic electrodes.

Figure 10 shows a photograph of the proposed miniature filter device (measuring about 2700 × 700 microns).

A local section in the filter device is shown in figure 11.

The substrate contains spatial electrodes (visible through the partial structure). Differential actuation [5] was used to drive each individual degree of freedom.

The equations of motion describing the five DOF device are

$$\begin{pmatrix} m_1 & 0 & 0 & 0 & 0 \\ 0 & m_2 & 0 & 0 & 0 \\ 0 & 0 & m_3 & 0 & 0 \\ 0 & 0 & 0 & m_2 & 0 \\ 0 & 0 & 0 & 0 & m_1 \end{pmatrix} \begin{pmatrix} \ddot{\varphi}_1 \\ \ddot{\varphi}_2 \\ \ddot{\varphi}_3 \\ \ddot{\varphi}_4 \\ \ddot{\varphi}_5 \end{pmatrix}$$

$$+ \begin{pmatrix} k_1 + k_2 & -k_2 & 0 & 0 & 0 \\ -k_2 & k_2 + k_3 & -k_3 & 0 & 0 \\ 0 & -k_3 & k_3 + k_3 & -k_3 & 0 \\ 0 & 0 & -k_3 & k_3 + k_2 & -k_2 \\ 0 & 0 & 0 & -k_2 & k_2 + k_1 \end{pmatrix} \begin{pmatrix} \varphi_1 \\ \varphi_2 \\ \varphi_3 \\ \varphi_4 \\ \varphi_5 \end{pmatrix} = \begin{pmatrix} Q_1 \\ Q_2 \\ Q_3 \\ Q_4 \\ Q_5 \end{pmatrix}, \quad (12)$$

where  $\mathbf{Q}$ ,  $\varphi$  represent a vector of five moments and angular displacements, respectively.

The mass and the stiffness coefficients are computed by solving the inverse eigenvalue problem which is explained theoretically in [20, 21]. The mass and stiffness elements had

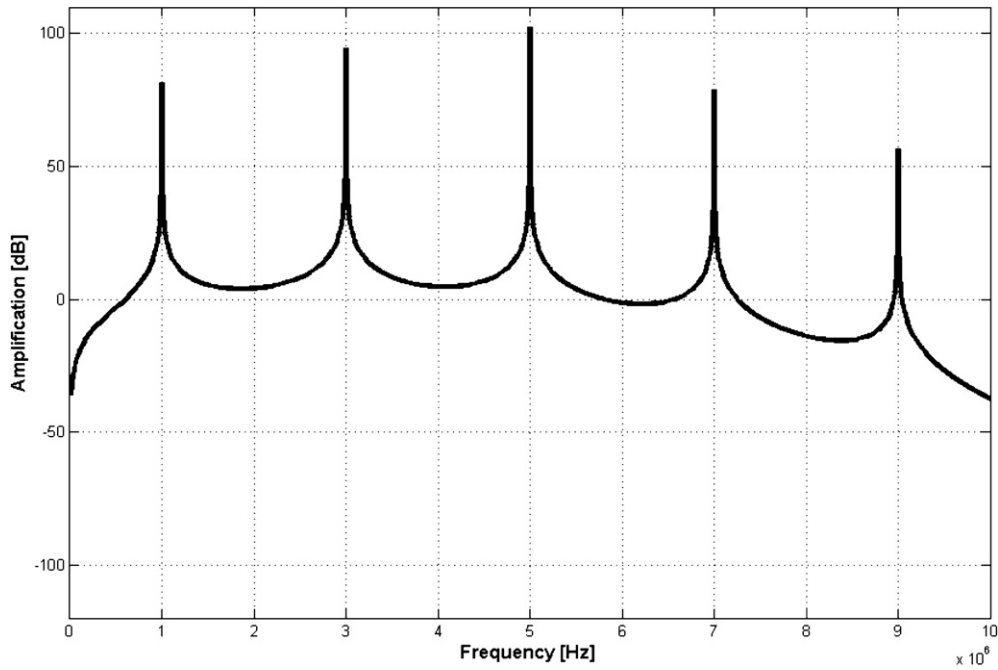


Figure 9. High- $Q$  multiple selective filter for odd frequencies.

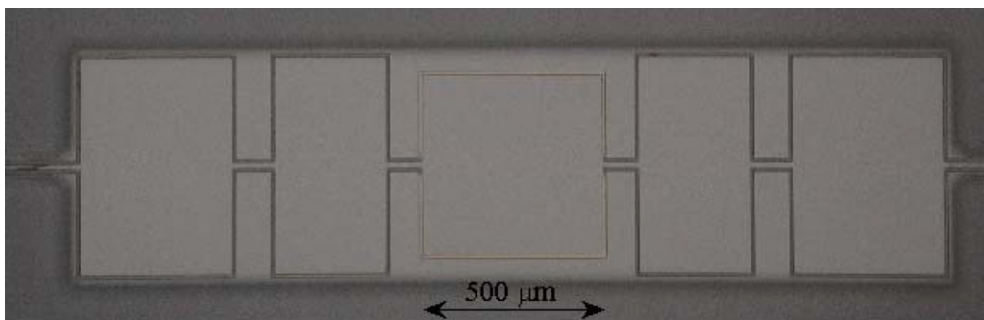


Figure 10. Upper view photograph of the MEMS filter under a microscope.



Figure 11. Local section in the filter device.

nominal, unscaled values of

$$\begin{aligned} (m_1 \ m_2 \ m_3) &= \alpha(20 \ 15 \ 14), \\ (k_1 \ k_2 \ k_3) &= \beta(10 \ 18 \ 21). \end{aligned} \tag{13}$$

These values can all be scaled to obtain a basis frequency of 13 kHz by choosing  $\frac{\beta}{\alpha} = 5(2\pi \cdot 13\,000)^2$ .

The translation of the stiffness and mass values from the lumped model to physical dimensions is carried out by standard formulae [23], neglecting the warping function correction [24] for the estimate of the torsional spring stiffness. The torsional spring stiffness was defined according to

$$k_i = \frac{cGh^3t}{L_i} \quad i = 1, 2, 3, \tag{14}$$

and the mass moment of inertia is equal to

$$m_i = \frac{a_i b_i t \rho (b_i^2 + t^2)}{12} \quad i = 1, 2, 3, \tag{15}$$

where  $h$  is defined as beam cross section thickness,  $t$  is defined as beam cross section width,  $G$  is defined as shear modulus,  $L_i$  is defined as beam length,  $c$  is defined as numerical factor depending on the ratio  $h/t$ ,  $\rho$  is defined as density,  $a_i$  is defined as inertia length (parallel to the rotation axis) and  $b_i$  is defined as width of the  $i$ th mass (perpendicular to the rotation axis)

A better accuracy for the geometrical dimensions can be obtained by optimizing a three-dimensional finite-element

**Table 1.** Geometrical parameters of the MEMS filter in  $\mu\text{m}$  (see equations (14) and (15)).

	Mass dimension = $a_i b_i$	Spring dimension = $L_i h$
$i = 1$	$500 \times 500$	$101 \times 15$
$i = 2$	$309 \times 600$	$117 \times 15$
$i = 3$	$411 \times 600$	$211 \times 15$

model [16]. The effect of the manufacturing process on the geometrical tolerances cannot be underestimated. Due to the geometrical imperfections, caused by the manufacturing process, the vibrating structure will not perfectly match the frequencies required and thus impose on the filter specification [16]. This calculation process has resulted in a vibrating device acting as a filter for periodic signals.

The nominal values of the geometrical parameters of the MEMS filter device are summarized in table 1.

The thickness of the device is  $t = 50 \mu\text{m}$ .

#### 4.1. Fabrication process

The MEMS filter device shown in figure 10 was designed according to an established process, consisting of a device die and a substrate die assembled together in a flip chip process [25, 26]. A SOI wafer consisting of a  $50 \mu\text{m}$  device layer, a  $350 \mu\text{m}$  handle layer and a  $2 \mu\text{m}$  box layer was micro-machined by the following four main steps:

*Step 1:* Deposition of  $2000 \text{ \AA}$  thick gold pads on the device layer for assembly purposes and serving as electrical connections to the filter structure.

*Step 2:* DRIE process on the handle side was used in order to free the filter structure from the handle layer and to enable optical access.

*Step 3:* Etching of the oxide layer is used to free the structure from the oxide layer.

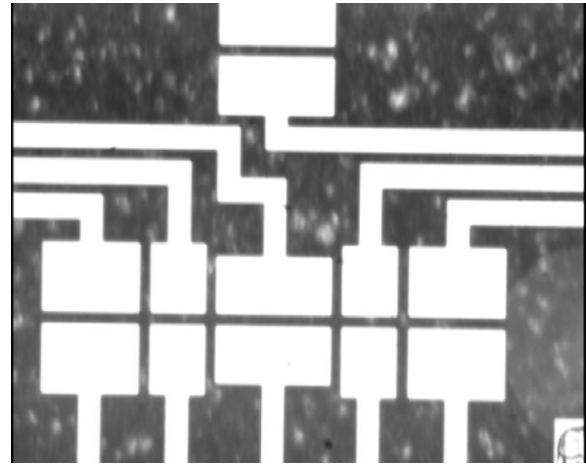
*Step 4:* DRIE process on the device side is used in order to free the filter structure from the device layer thus completing its mechanical release and enabling it to vibrate freely.

The substrate die layout is shown in figure 12.

The fabrication of the substrate consisted of a deposition of  $2000 \text{ \AA}$  thick nickel–chrome–gold electrodes. This layer was used both for the electrostatic actuation of the filter and also as a seed layer for the nickel electroplating, implemented in order to create a highly conductive spacer. This spacer allowed determining a gap of  $15 \mu\text{m}$  between the electrodes and the filter structure.

#### 4.2. Experimental set-up

The experimental set-up consisted of a laser vibrometer with a displacement/velocity sensor, a multi-channel, 16 bit data-acquisition system sampling at a rate of  $200 \text{ kHz}$ , oscilloscope sampling at a rate of  $12 \text{ MHz}$  and a vacuum chamber. The vacuum pressure during the measurements was  $0.0427 \text{ Torr}$ . Using an optical microscope and a transparent window in the chamber, the measuring laser beam is reduced to a diameter

**Figure 12.** Substrate photograph under microscope.

of about  $5 \mu\text{m}$ . The laser beam was located near the edge of the measured mass far from the rotation axis, thus attaining maximum sensitivity in the rotational mode of motion. On each of the two electrodes implanted on the substrate, an equal dc voltage  $15 \text{ V}$  with opposite potentials was applied. The device layer, which the filter structure is part of, was subjected to an ac voltage  $1 \text{ V}_{\text{pp}}$  at the excitation frequency.

#### 4.3. Experimental results

We measured the response of the MEMS filter device for several operational configurations and the FRF results were as expected and resembled the ones shown in the filter simulation. The base frequency for all the configurations was designed to be  $\omega_0 = 13 \text{ kHz}$ .

*4.3.1. Experiment 1. Response for actuation and sensing on centre of mass.* The actuation and sensing of the MEMS filter structure is on the central mass ( $m_3$ ) performed by separate parallel electrodes and a laser vibrometer, respectively. The frequency response function (FRF) amplitude is shown in figure 13.

Figure 13 shows that the structure behaved according to the abovementioned theory with the exception of a tiny spike near  $40 \text{ kHz}$ , caused by a bending mode of vibration which was excited by imperfections in the device and small damping [14]. Indeed, the design has a large amplification of the excitation voltage at frequencies  $\omega_0, 3\omega_0, 5\omega_0$  and an extremely high attenuation at  $2\omega_0, 4\omega_0, 6\omega_0$ .

*4.3.2. Experiment 2. Response for actuation on first mass and sensing on last.* The actuation of the MEMS filter structure, in this case, is on the first mass ( $m_1$ ) and it is performed by two separate parallel electrodes while the laser vibrometer senses the response of the last mass ( $m_5$ ). The measured FRF is shown in figure 14.

A typical response of this filter is observed, like an all pole filter. This configuration excites all the natural frequencies of

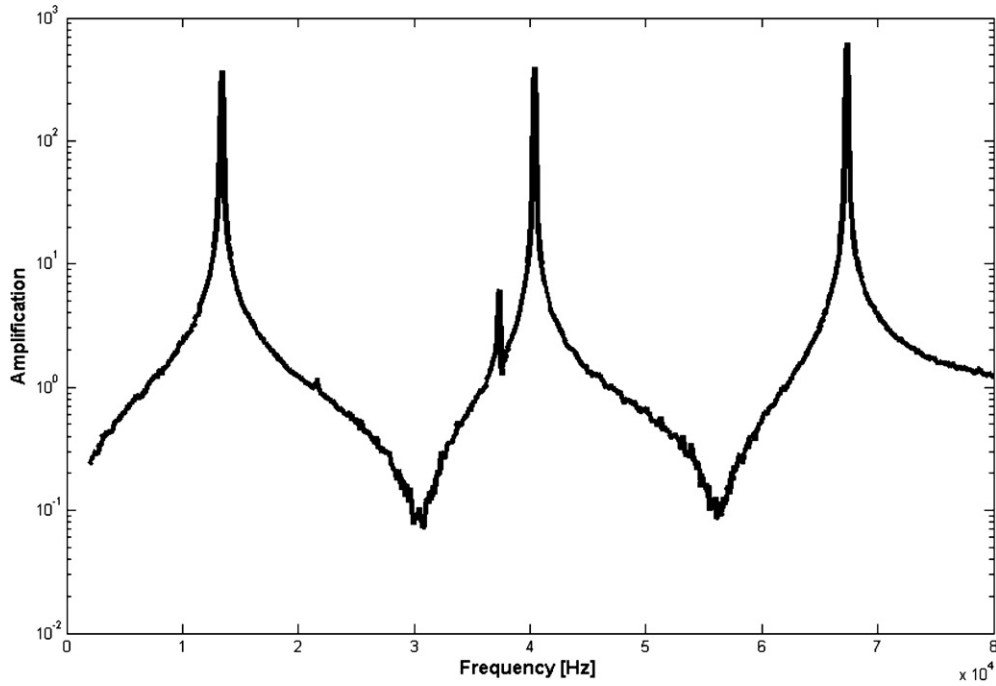


Figure 13. Response magnitude of the central mass in a five DOF system (measured).

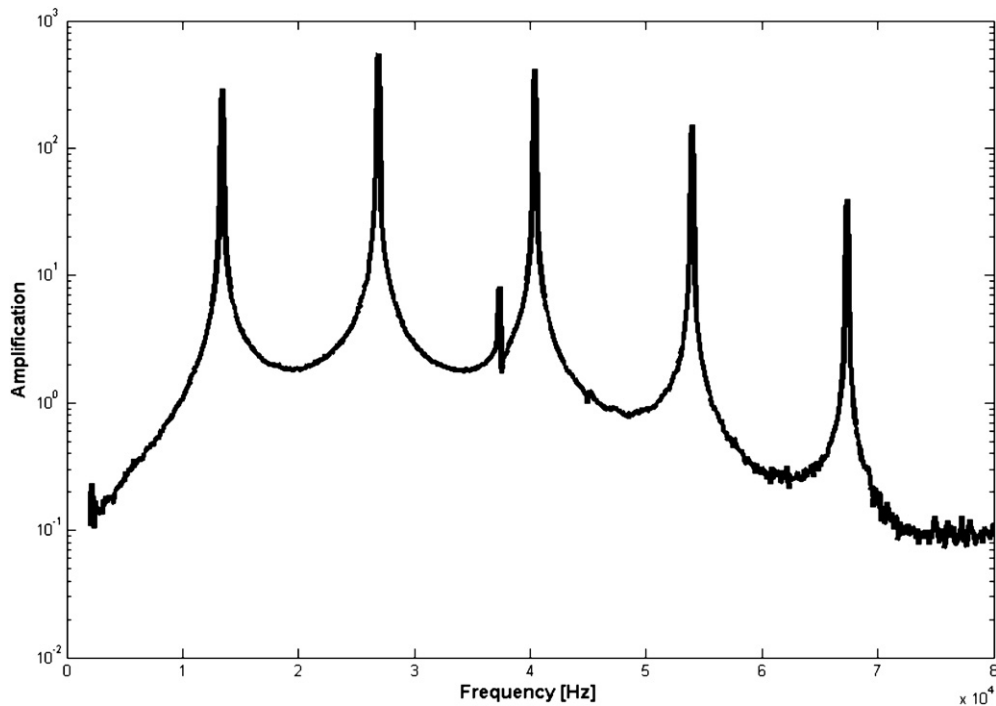


Figure 14. High- $Q$  multiple selective filter (measured).

this device. The design has a large amplification at integer multiples of the basis frequency, i.e. at  $n\omega_0$   $n = 1, \dots, 5$ .

The  $Q$  of the filter is of the order 1000; therefore the pass-band consists of distinct peaks serving as a narrow bandpassing filter for periodic signals.

4.3.3. Experiment 3. Response for actuation on first mass and sensing on the central mass. In the last experiment, the actuation of the structure was on the first mass ( $m_1$ ) while

sensing took place on the central mass ( $m_3$ ). The FRF is shown in figure 15.

The design configuration has a large amplification at odd frequencies  $\omega_0, 3\omega_0, 5\omega_0$ .

From a comparison between the simulated response (figure 9) and the measured response, it can be seen that the MEMS filter behaves as predicted, thus confirming that this type of filter operates according to what was suggested.

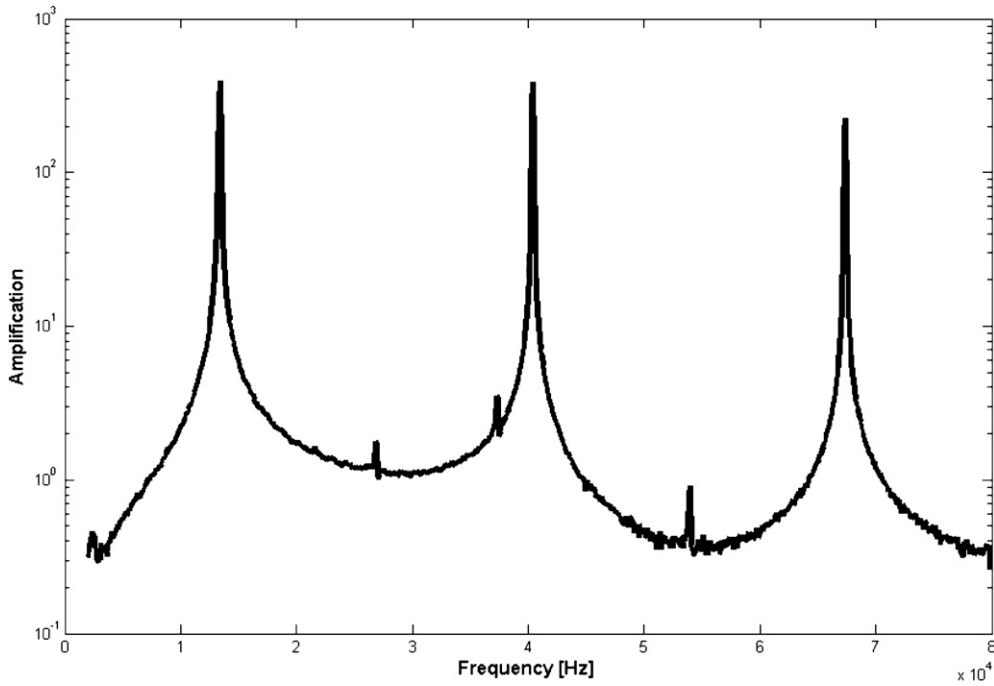


Figure 15. High-Q multiple selective filter for odd frequencies (measured).

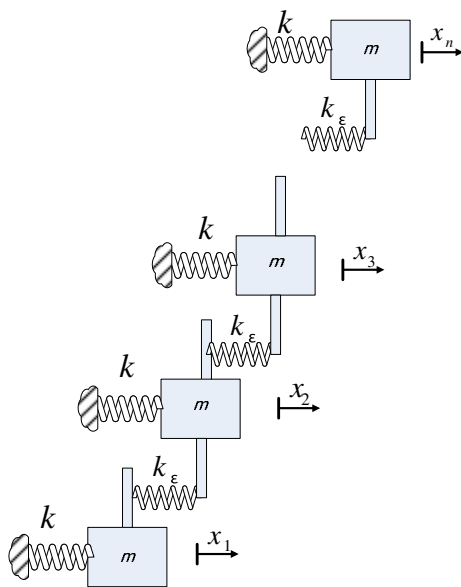


Figure 16. A MDOF enhanced system.

### 5. Controlling the bandwidth of a pass-band filter

This section deals with the accurate assignment of a cluster of natural frequencies as a means to control the bandwidth of an electromechanical filter [27]. The previously proposed topology is sensitive to the location of the natural frequencies whose values affect the shaping of the device’s frequency response. A solution with a modified topology seeking to minimize the effect of manufacturing tolerances and frequency drift is proposed. The band widening is created by assigning multiple natural frequencies in close proximity.

A new topology that allows us to design such structures will be presented from a structural vibration point of view.

Once we add an optimal amount of dissipation by adding damping to the system, we can obtain a flattened response in the pass-band.

#### 5.1. Proposed topology for a controlled bandwidth filter

So far, several configurations have been synthesized and studied in this paper. Here, a new, multi-degree of freedom system with enhanced selectivity on the spectrum is proposed. The overall suggested topology is shown in figure 16.

The ‘building block’ consists of single degree of freedom systems having mass  $m$  and spring stiffness  $k$ , which are coupled through a relatively weak coupling spring  $k_\epsilon$  to the adjacent subsystems. The coupling spring affects the bandwidth of the pass-band, thus spectral shaping can be achieved.

The equation of motion for the enhanced system is [28]

$$\begin{bmatrix} m & & & & \\ & m & & & \\ & & \ddots & & \\ & & & \ddots & \\ & & & & m \end{bmatrix} \begin{Bmatrix} \ddot{x}_1 \\ \ddot{x}_2 \\ \vdots \\ \vdots \\ \ddot{x}_N \end{Bmatrix} + \begin{bmatrix} k & & & & \\ & k & & & \\ & & \ddots & & \\ & & & \ddots & \\ & & & & k \end{bmatrix} \begin{Bmatrix} x_1 \\ x_2 \\ \vdots \\ \vdots \\ x_N \end{Bmatrix} + k_\epsilon \begin{bmatrix} 1 & -1 & & & \\ -1 & 2 & -1 & & \\ & -1 & \ddots & \ddots & \\ & & \ddots & 2 & -1 \\ & & & -1 & 1 \end{bmatrix} \begin{Bmatrix} x_1 \\ x_2 \\ \vdots \\ \vdots \\ x_N \end{Bmatrix} = 0. \quad (16)$$

Substituting the assumed sinusoidal solution at steady state  $x = x_0 e^{j\omega t}$  in (16) and normalizing (16) by the spring stiffness,

one obtains

$$-\left(\frac{\omega}{\omega_0}\right)^2 \begin{bmatrix} 1 & & & & \\ & 1 & & & \\ & & \ddots & & \\ & & & \ddots & \\ & & & & 1 \end{bmatrix} \{x_0\} + \begin{bmatrix} 1 & & & & \\ & 1 & & & \\ & & \ddots & & \\ & & & \ddots & \\ & & & & 1 \end{bmatrix} \{x_0\} + \frac{k_\varepsilon}{k} \begin{bmatrix} 1 & -1 & & & \\ -1 & 2 & -1 & & \\ & -1 & \ddots & \ddots & \\ & & \ddots & 2 & -1 \\ & & & -1 & 1 \end{bmatrix} \{x_0\} = 0. \quad (17)$$

The natural frequency of a single DOF system ‘building block’ is defined by [29]

$$\omega_0^2 = \frac{k}{m}. \quad (18)$$

Using the former definitions in (17), a normalized set of equations is formed, where

$$\mathbf{B} = \begin{bmatrix} 1 & -1 & & & \\ -1 & 2 & -1 & & \\ & -1 & \ddots & \ddots & \\ & & \ddots & 2 & -1 \\ & & & -1 & 1 \end{bmatrix}.$$

A symmetric, tri-diagonal Jacobi matrix

$$\Delta k \triangleq \frac{k_\varepsilon}{k}, \quad \sigma_i^2 \triangleq \left(\frac{\omega}{\omega_0}\right)^2$$

and the eigenvalues of (17) are

$$\sigma^2 \triangleq \begin{bmatrix} \sigma_1^2 & & & \\ & \sigma_2^2 & & \\ & & \ddots & \\ & & & \sigma_n^2 \end{bmatrix}. \quad (19)$$

Indeed, equation (17) can be recast in a generalized eigenvalue problem  $\mathbf{K}\phi = \omega^2\mathbf{M}\phi$  form [29],

$$[\mathbf{I} + \mathbf{B}\Delta k] \phi = \sigma^2 \phi, \quad (20)$$

or

$$\Delta k \mathbf{B}\phi = (\sigma^2 - 1)\phi$$

and

$$\mathbf{B}\phi = \frac{(\sigma^2 - 1)}{\Delta k} \phi. \quad (21)$$

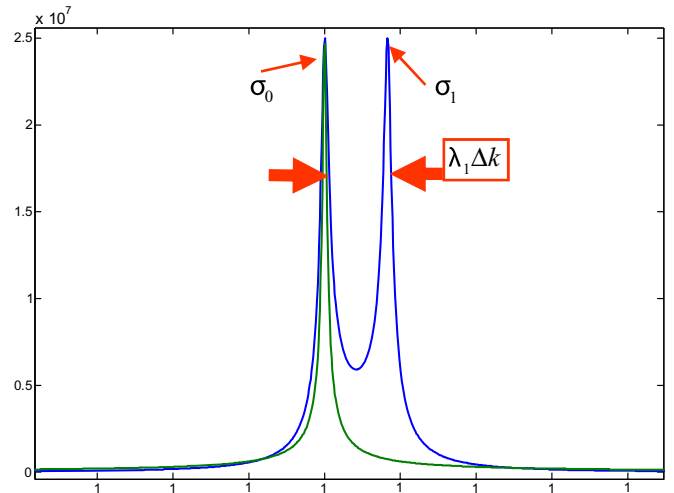


Figure 17. A two resonators system.

Defining the eigenvectors  $\mathbf{V}$  of the matrix  $\mathbf{B}$ , it is clear that

$$\mathbf{V}^T \mathbf{B} \mathbf{V} = \lambda = \begin{bmatrix} \lambda_1 & & \\ & \ddots & \\ & & \lambda_n \end{bmatrix}, \quad (22)$$

where  $\lambda$  are the eigenvalues of the matrix  $\mathbf{B}$ .

The matrix  $[\mathbf{I} + \mathbf{B}\Delta k]$  is symmetric, thus the modes  $\{\phi_i\}$  are orthogonal and hence the eigenvectors of matrix  $\mathbf{B}$  are orthonormal, i.e.  $\mathbf{V}^T \mathbf{V} = \mathbf{I}$ .

After performing some algebraic manipulations on (21) it can be seen that

$$\mathbf{V}^T \mathbf{B} \mathbf{V} = \frac{(\sigma^2 - 1)}{\Delta k} = \lambda. \quad (23)$$

The solution of the eigenvalue problem, equation (20), can be simplified into

$$\sigma_i^2 = 1 + \Delta k \mathbf{V}_i^T \mathbf{B} \mathbf{V}_i. \quad (24)$$

From (22), we have that

$$\lambda_i \triangleq \mathbf{V}_i^T \mathbf{B} \mathbf{V}_i. \quad (25)$$

Thus the eigenvalue solution derived from (24) can be rewritten as

$$\sigma_i^2 = 1 + \lambda_i \Delta k. \quad (26)$$

For example, we can use (18) to design a system with two resonators, as shown in figure 17.

Assuming that  $\Delta k = 1$ , this system has two natural frequencies, according to (26), the first frequency is  $\sigma_0^2 = 1$  and the second frequency is  $\sigma_1^2 = 1 + \lambda_1 \Delta k = 1.7321$ .

It was demonstrated that the spectral bandwidth can be controlled by setting the number of adjacent systems and their coupling springs.

### 5.2. Controlling the interval of the frequency bandwidth

In order to control the bandwidth to have a constant shift in the natural frequencies, we need to select and calculate different coupling springs. This type of problem belongs to the class of inverse problems [20, 21].

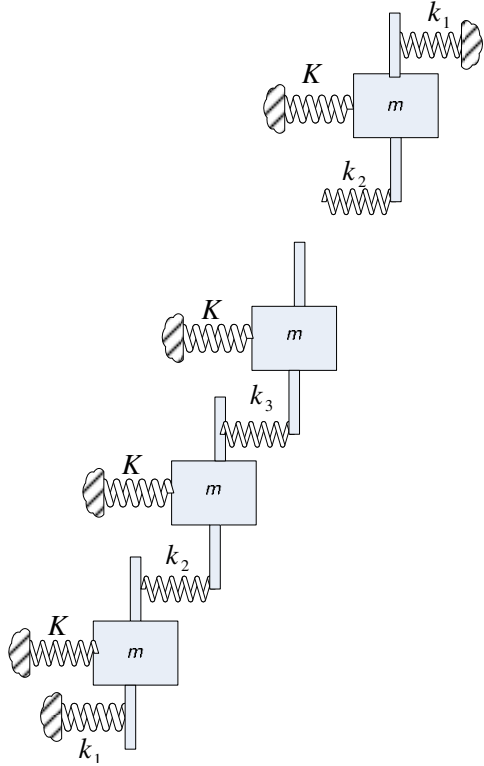


Figure 18. Connecting subsystems of springs.

A new topology that enables us to perform precise bandwidth control is proposed here. The system's topology is schematically illustrated in figure 18, the 'building block' of a spring-mass consists of a single DOF that is connected with low coupling independent springs  $k_i$  and an additional two ground springs that connect the first and last masses.

The same theory of [20, 21] is being used to design the subsystem of coupling springs vibrating system with an assigned spectrum.

The system has  $n = (2N - 1)$  degrees of freedom and it is symmetric around the central mass. The symmetry of the proposed topology defines that  $k_i = k_{2N-i+1}$ ,  $i = 1, \dots, N$ .

Its dynamical behaviour and the values of the individual coupling springs can be determined by solving the eigenvalue problem of the tri-diagonal Jacobian matrix.

The equation of motion for the vibrating system shown in figure 18 is

$$-\omega^2 \begin{bmatrix} m & & & \\ & m & & \\ & & \ddots & \\ & & & m \end{bmatrix} \{x_0\} + \left( \begin{bmatrix} k & & & \\ & k & & \\ & & \ddots & \\ & & & k \end{bmatrix} + [\mathbf{B}] \right) \{x_0\} = 0. \quad (27)$$

The weak coupling springs are treated as a subsystem defined by matrix  $\mathbf{B}$  which is a symmetric, tri-diagonal Jacobian matrix

$$\mathbf{B} = \begin{bmatrix} k_1 + k_2 & -k_2 & & \\ -k_2 & k_2 + k_3 & & \\ & & \ddots & \ddots \\ & & & \ddots & \ddots \end{bmatrix}.$$

Normalizing (27) by the spring stiffness, one obtains

$$-\left(\frac{\omega}{\omega_0}\right)^2 \begin{bmatrix} 1 & & & \\ & 1 & & \\ & & \ddots & \\ & & & 1 \end{bmatrix} \{x_0\} + \left( \begin{bmatrix} 1 & & & \\ & 1 & & \\ & & \ddots & \\ & & & 1 \end{bmatrix} + \frac{1}{k} [\mathbf{B}] \right) \{x_0\} = 0. \quad (28)$$

The natural frequency of a single DOF system 'building block' is defined by [29]

$$\omega_0^2 = \frac{k}{m} \quad (29)$$

and the natural frequencies of the enhanced system are

$$\sigma_i^2 = \left(\frac{\omega_i}{\omega_0}\right)^2 \quad i = 1, \dots, n.$$

Equation (28) can be recast in a generalized eigenvalue problem  $\mathbf{K}\phi = \omega^2\mathbf{M}\phi$  form:

$$\left[ \mathbf{I} + \frac{1}{k} \mathbf{B} \right] \phi = \sigma^2 \phi. \quad (30)$$

Defining

$$\tilde{\mathbf{B}} = \frac{1}{k} \mathbf{B},$$

one obtains

$$\tilde{\mathbf{B}}\phi = (\sigma^2 - 1)\phi. \quad (31)$$

Using  $\mathbf{V}$ , the eigenvectors of the matrix  $\tilde{\mathbf{B}}$ , it is clear that

$$\mathbf{V}^T \tilde{\mathbf{B}} \mathbf{V} = \lambda = \begin{bmatrix} \lambda_1 & & \\ & \ddots & \\ & & \lambda_n \end{bmatrix}. \quad (32)$$

And since the eigenvectors are orthonormal and after performing some algebraic manipulations on (31), we can obtain

$$\mathbf{V}^T \tilde{\mathbf{B}} \mathbf{V} = (\sigma^2 - 1) = \lambda, \quad (33)$$

where  $\lambda$  are the eigenvalues of the matrix  $\tilde{\mathbf{B}}$ . Each eigenvalue  $\lambda$  is associated with a particular pole/zero.

The solution for the eigenvalue problem, equation (30), can be simplified into

$$\sigma_i^2 = 1 + \mathbf{V}_i^T \tilde{\mathbf{B}} \mathbf{V}_i. \quad (34)$$

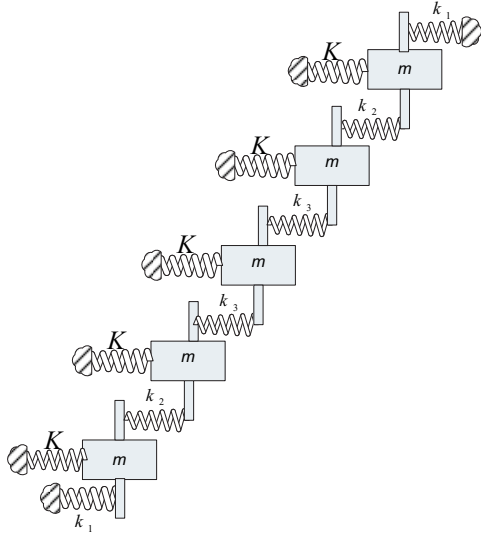


Figure 19. Symmetric five DOF vibrating system.

From (33), we have that

$$\lambda_i \triangleq \mathbf{V}_i^T \tilde{\mathbf{B}} \mathbf{V}_i. \quad (35)$$

Thus the eigenvalue solution derived from (34) can be rewritten as

$$\sigma_i^2 = 1 + \lambda_i. \quad (36)$$

Define a constant shift parameter  $\omega_s$  between the natural frequencies of the enhanced system

$$\omega_s = \sigma_{i+1} - \sigma_i = \text{Const} \quad i = 1, \dots, n.$$

Thus

$$\sigma_i^2 = \left(\frac{\omega_i}{\omega_0}\right)^2 \Rightarrow \sigma_i = \left(\frac{\omega_i}{\omega_0}\right) = 1 + (i - 1) \omega_s. \quad (37)$$

For the general case using equation (36), we define

$$\omega_s = \sqrt{1 + \lambda_{i+1}} - \sqrt{1 + \lambda_i}. \quad (38)$$

From (38), we get

$$\lambda_{i+1} = \omega_s^2 + 2\omega_s\sigma_i + \sigma_i^2 - 1. \quad (39)$$

These are the eigenvalues of the Jacobian matrix  $\tilde{\mathbf{B}}$ .

Substituting (37) in (39), we obtain

$$\lambda_{i+1} = \omega_s^2 + (1 + (i - 1) \omega_s) (1 + (i + 1) \omega_s) - 1. \quad (40)$$

Matrix  $\tilde{\mathbf{B}}$  is thus singular, and the first eigenvector of  $\tilde{\mathbf{B}}$  is related to  $\lambda_1 = 0$ .

The topology of the subsystem is found by employing the same algorithm yet again [20] such that a system is reconstructed to have a specified spectrum [22]. An example of a symmetric five DOF vibrating system will be used to demonstrate the new filter synthesis methodology in figure 19.

The actuation, in this example, is on the first mass and sensing is on the last mass. The result for this system is shown in figure 20.

Figure 20 shows the precisely tuned frequency bandwidth compared with a single DOF system. Zooming on figure 20, the effect of the constant shift parameter  $\omega_s$  between the resonances can be seen. In this example  $\omega_s = 0.02$  [Hz] was used, and the result, shown in figure 21, clearly shows that this is indeed the case.

Once we add an optimal amount of dissipation by adding dampers to the system, we can obtain a flattened bandpass, shown as the thick black line in figure 21. The bandwidth of

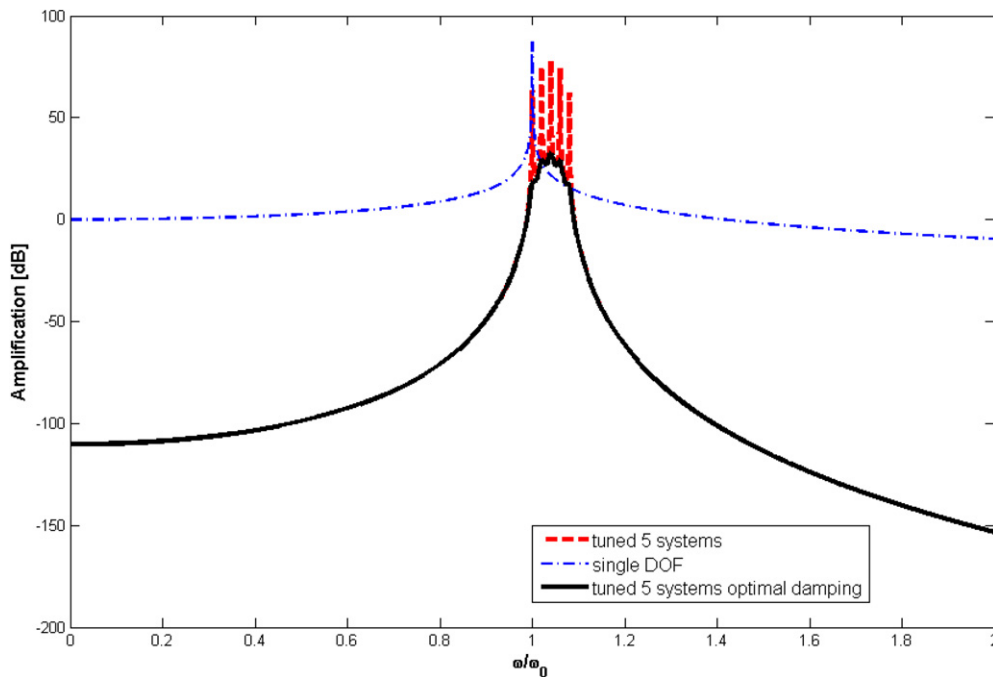
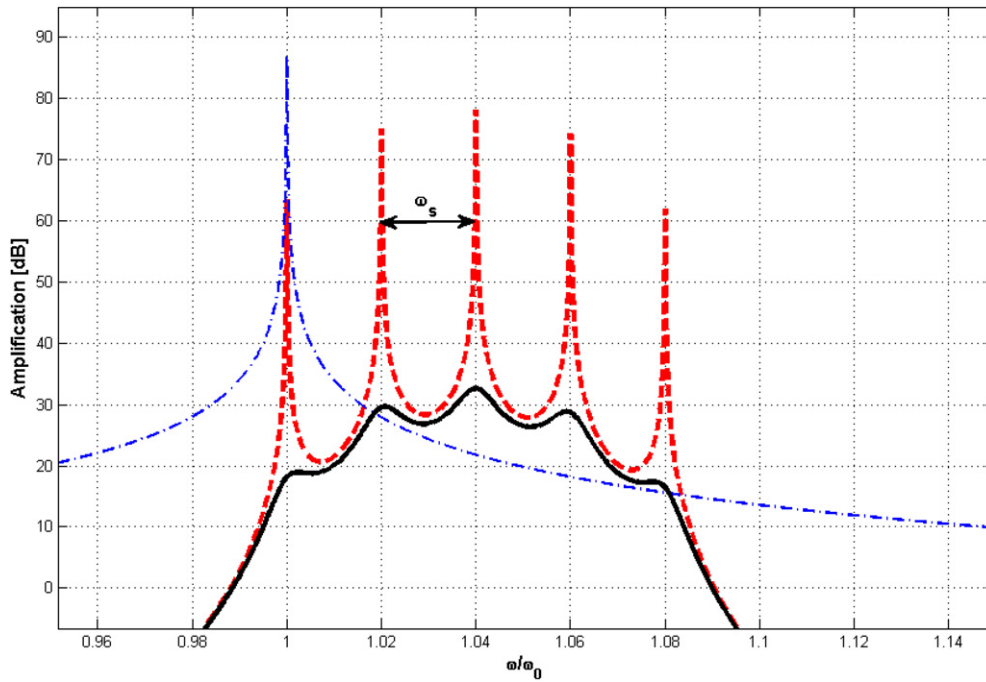
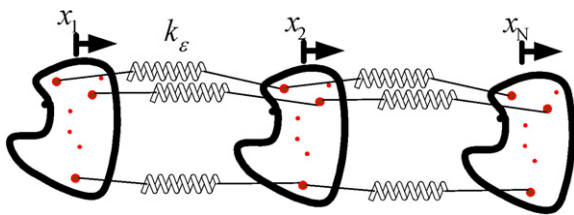


Figure 20. Uniformly spaced natural frequencies for an increased bandwidth.



**Figure 21.** Uniformly spaced natural frequencies for increased bandwidth—zoomed (red: undamped, black: with damping, blue: single dof system)



**Figure 22.** Connecting  $N$  identical systems.

the filter was enhanced precisely by adding several degrees of freedom and choosing appropriate coupling springs.

*5.3. Enhanced model topology synthesis—possible extension to a lattice system*

A natural extension to the former analysis would replace the single DOF system ‘building block’ with a multi-DOF system ‘building blocks’ having the same masses and springs. These systems will be coupled through a relatively weak coupling spring  $k_ε$  to the adjacent system; this assures that the natural frequencies and anti-resonance frequencies will have a sufficient width to accommodate manufacturing tolerances.

In general, there are  $N$  identical systems connected with weak coupling springs, as shown in figure 22.

*5.3.1. Example of filter with enhanced topology—lattice system.* As an example of a typical system three ‘building blocks’ each consisting of a five mass system with equal weak coupling springs is proposed. The systems and the connecting springs are shown in figure 23.

This compound system is in fact symmetric around the middle building block and thus it has symmetric and anti-symmetric modes of vibration [21]. There are structural modes where all the ‘building blocks’ move in unison, while there are anti-symmetric ones for which each building block has nearly the same vibration mode but the weak coupling springs, through the anti-symmetric motion, causes a slight frequency shift causing a peak in the frequency response whose shift is determined by the weak coupling springs. This phenomenon is used to widen the bandpass filter’s response around the natural frequencies.

The frequency response of this compound system is shown in figure 24. In this case, the actuation is on the central mass of the first system and the sensing is on the central mass of the last system.

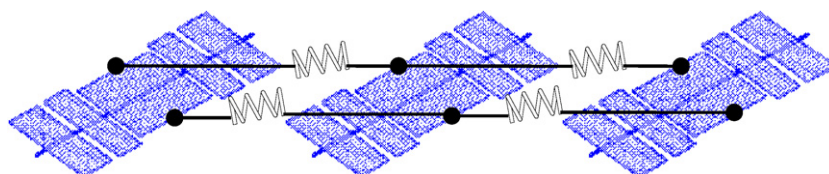


**Figure 23.** Example of connecting three identical systems.

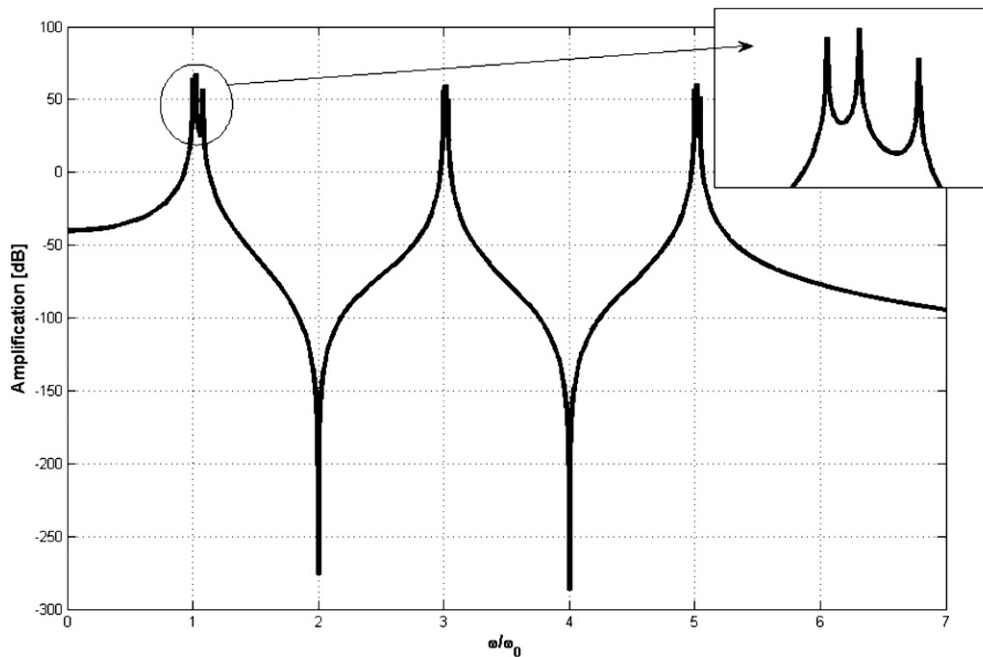


Figure 24. FRF of a lattice system.

A close examination of the peaks near the natural frequencies shows multiple peaks whose number corresponds to the number of building blocks being used. As before, it is evident that the concept of periodic signal filtering can now be enhanced with the proposed topology by widening the individual pass-bands in a controlled manner.

## 6. Conclusion

This paper introduces some new ideas for the construction of mechanical filters alongside new topologies while developing a synthesis methodology taken from structural dynamics. An approach relying on basic mechanics recognizes the contribution of individual mechanical modes of vibration and thus creates several variants of a mechanical filter.

It was demonstrated with a new method that a narrow band filter's width can be precisely controlled by connecting several identical structures together and by assigning natural frequencies of the coupling system.

## References

- [1] Yao J J 2000 Topical review RF MEMS from a device perspective *J. Micromech. Microeng.* **10** R9–38
- [2] Mason W P 1948 *Electromechanical Transducers and Wave Filters* (New York: Van Nostrand Reinhold)
- [3] Lin L, Howe R T and Pisano A P 1998 Microelectromechanical filters for signal processing *J. Microelectromech. Syst.* **7** 3
- [4] Johnson R A 1983 *Mechanical Filters in Electronics* (New York: Wiley)
- [5] Bao M H 2000 *Handbook of Sensors and Actuators Micro Mechanical Transducers: Pressure Sensors, Accelerometers and Gyroscopes* vol 8 (Amsterdam: Elsevier)
- [6] Wang K and Nguyen C T C 1999 High-order medium frequency micromechanical electronic filters *J. Microelectromech. Syst.* **8** 534–56
- [7] Bannon F D, Clark J R and Nguyen C T C 2000 High-Q HF microelectromechanical filters *IEEE J. Solid-State Circuits* **35** 512–26
- [8] Temes G C and Mitra S K 1973 *Modern Filter Theory and Design* (New York: Wiley)
- [9] Hsu W-T, Clark J R and Nguyen C T C 2000 Mechanically temperature compensated flexural mode micromechanical resonators *Technical Digest of IEEE Int. Electron Devices Meeting (San Francisco, Los Angeles)* pp 399–402
- [10] Demirci Mustafa U and Nguyen Clark C T C 2005 Single resonator fourth order micromechanical disk filters *Proc. 18th Int. IEEE Micro Mechanical Systems Conf. (Miami, FL)* pp 207–10
- [11] Clark R, Hsu W-T and Nguyen C T C 2000 High-Q VHF micromechanical contour-mode disk resonators *IEEE Int. Electron Devices Meeting* pp 399–402
- [12] Greywell D S and Busch P A 2002 Coupled micromechanical drumhead resonators with practical applications as electromechanical bandpass filters *J. Micromech. Microeng.* **12** 925–38
- [13] Li S-S, Lin Y-W, Ren Z and Nguyen Clark C T C 2005 Self-switching vibrating micromechanical filter bank *Proc. Joint IEEE Int. Frequency Control/Precision Time & Time Interval Symp. (Vancouver, Canada)* pp 135–141
- [14] Minikes A, Bucher I and Avivi G 2005 Damping of a micro-resonator torsion mirror in rarefied gas ambient *J. Micromech. Microeng.* **15** 1762–9
- [15] Tilmans H A C 1996 Equivalent circuit representation of electromechanical transducers: I. Lumped parameter system *J. Micromech. Microeng.* **6** 157–76
- [16] Avivi G and Bucher I 2008 A method for eliminating the inaccuracy of natural frequency multiplications in a multi DOF micro scanning mirror *J. Micromech. Microeng.* **18**
- [17] Bucher I and Braun S G 1994 Efficient optimization procedure for minimizing the vibratory response via redesign or modification, part I. Theory *J. Sound Vib.* **175** 433–54
- [18] Bucher I and Braun S G 1993 The structural modification inverse problem: an exact solution *Mech. Syst. Signal Process.* **7** 217–38

- [19] Bucher I, Zimmerman Y, Velger M and Erlich R 2004 Design and analysis of a multi-DOF micro-mirror for triangular wave scanning *J. Mech. Behav. Mater.* **14** 369–82
- [20] Bucher I 2008 A mechanical Fourier series generator—an exact solution *J. Vibrat. Acoust.* at press
- [21] Gladwell G M L 1986 *Inverse Problems in Vibration* (Dordrecht: Nijhoff)
- [22] Parlett B 1980 *The Symmetric Eigenvalue Problem* (Englewood Cliffs, NJ: Prentice-Hall)
- [23] Timoshenko S P and Goodier J N 1970 *Theory of Elasticity* 3rd edn (New York: McGraw-Hill)
- [24] Basler K and Kollbrunner C F 1969 *Torsion in Structures* (New York: Springer)
- [25] Madou M J 2002 *Fundamentals of Microfabrication: The Science of Miniaturization* (Boca Raton, FL: CRC Press)
- [26] Maluf N 2000 *Introduction to Microelectromechanical Systems Engineering* (Boston, MA: Artech House)
- [27] Elka A 2007 A synthesis and modeling approach for micro-electromechanical filters using structural dynamics *PhD Thesis* Technion—Israel Institute of Technology
- [28] Meirovitch L 1980 *Computational Methods in Structural Dynamics* (Rockville, MD: Sijthoff & Noordhoff)
- [29] Ewins D J 1995 *Modal Testing: Theory and Practice* (New York: Wiley)